A 3D model of tumour angiogenic microenvironment to monitor hypoxia effects on cell interactions and cancer stem cell selection

Krzysztof Klimkiewicz, Kazimierz Weglarczyk, Guillaume Collet, Maria Paprocka, Alan Guichard, Michal Sarna, Alicja Jozkowicz, Jozef Dulak, Tadeusz Sarna, Catherine Grillon, et al.

Cancer Letters 396 (2017) 10–20

Contents lists available at ScienceDirect

Cancer Letters

journal homepage: www.elsevier.com/locate/canlet

Original Article

A 3D model of tumour angiogenic microenvironment to monitor hypoxia effects on cell interactions and cancer stem cell selection

Krzysztof Klimkiewicz [a, b], Kazimierz Weglarczyk [a, 1], Guillaume Collet [a, 2], Maria Paprocka [c], Alan Guichard [a], Michal Sarna [b], Alicja Jozkowicz [d], Jozef Dulak [d, e], Tadeusz Sarna [b], Catherine Grillon [a], Claudine Kieda [a, e, *]

[a] Centre for Molecular Biophysics, UPR 4301 CNRS Affiliated to Orléans University and INSERM, Orléans Cedex 02, France
[b] Department of Biophysics, Faculty of Biochemistry, Biophysics and Biotechnology, Jagiellonian University, ul. Gronostajowa 7, 30387, Kraków, Poland
[c] Laboratory of Glycobiology and Cell Recognition, Ludwik Hirszfeld Institute of Immunology and Experimental Therapy, PAN, U. Rudolfa Weigla 12, 53114, Wrocław, Poland
[d] Department of Medical Biotechnology, Faculty of Biochemistry, Biophysics and Biotechnology, Jagiellonian University, ul. Gronostajowa 7, 30387, Kraków, Poland
[e] Malopolska Centre of Biotechnology, Jagiellonian University, ul. Gronostajowa 7A, 30-387, Krakow, Poland

ARTICLE INFO

Article history:
Received 31 January 2017
Received in revised form
1 March 2017
Accepted 3 March 2017

Keywords:
Angiogenesis
Endothelial progenitors
Hypoxia
microRNA
Recruitment
Spheroid tumour model

ABSTRACT

Tumour microenvironment determines the fate of treatments. Reconstitution of tumour conditions is mandatory for alternative *in vitro* methods devoted to cancer development and the selection of therapeutic strategies. This work describes a 3D model of melanoma growth in its environment. Introducing means to mimic tumour angiogenesis, which turns on tumour progression, the model shows that melanoma tumour spheroids allow reconstitution of solid tumours with stromal cells. Angiogenesis evidenced the differential recruitment of endothelial cells (EC) from early progenitors (EEPCs) to mature ECs. Hypoxia was the key parameter that selected and stabilized melanoma cancer stem like cells (CSCs) phenotype based on aldehyde dehydrogenase expression as the best criterion. The 3D-tumour-model demonstrated the distinct reactivity of ECs toward tumour cells in terms of cellular cross-talk and humoral response. Intra-spheroid cell-to-cell membrane dye exchanges, mediated by intercellular interactions, uncovered the melanoma-to-EEPC cooperation. The resulting changes in tumour milieu were evidenced by the chemokinic composition and hypoxia-related variations in microRNA expression assessed in each cellular component of the spheroids. This method brings new tools to decipher the molecular mechanism of tumour-mediated cell recruitment and for *in vitro* assessment of therapeutic approaches.

Introduction

Melanocytes are melanin-producing cells in response to ultraviolet (UV) radiations. Melanin forms in keratinocytes a photoprotective cap over the cell nucleus reducing DNA damage [1]. Intense and intermittent exposure of the skin to solar radiation, without proper protection can damage DNA leading to mutations and carcinogenesis [2]. Although melanoma represents only 4% of all skin cancers, it is responsible for the majority (70%) of skin-cancer related deaths [3]. Melanoma is a strongly metastatic [2], very heterogeneous, complex cancer which cannot be properly studied using classical *in vitro* culture methods. Critically important for adequate evaluation of the effectiveness of a therapy, are alternative *in vitro* methods with the ability to properly reproduce as much as possible the melanoma microenvironment that exists *in vivo*. Therefore technologies mimicking the three-dimensional tumour microenvironment are in great demand. 3D organotypic spheroid cultures in collagen-derived matrices may be viewed as alternative methods to validate and improve preclinical strategies [4].

* Corresponding author. Centre for Molecular Biophysics, UPR 4301 CNRS Affiliated to Orléans University and INSERM, Orléans Cedex 02, France.
E-mail address: claudine.kieda@cnrs-orleans.fr (C. Kieda).
[1] Department of Clinical Immunology, Institute of Paediatrics, Faculty of Medicine, Jagiellonian, University Medical College, ul. Wielicka 265, 30-663, Krakow, Poland.
[2] Department of Mineral and Analytical Chemistry, University of Geneva, CH-1211, Geneva 4.

http://dx.doi.org/10.1016/j.canlet.2017.03.006

A tumour as a complex pathologic tissue [5] is a concept of considerable consequences for treatments. This show the need to reconstitute such tissue conditions while setting *in vitro* alternative methods for application to cancer models *in vivo* [6]. Hypoxia occurs when a tumour develops. It turns on the angiogenic switch, stabilizing HIF-1α, the main transcription factor which controls the production of proangiogenic molecules as VEGFs by tumour cells. The angiogenic switch operates mainly on the tumour-surrounding ECs, making sprouting of vicinal vessels and also by recruitment of EPCs from the bone marrow to specifically reach the hypoxic regions in tumours [7], [8]. However, the tumour micro vessels remain abnormal and not functional to bring blood, consequently oxygen, into the tumour mass. This leads to a non-ending proangiogenic state which makes pathologic angiogenesis a hallmark of cancer [9–12].

In melanoma as in other tumours, cancer cells and microenvironment adapt mutually to optimize growth and invasion conditions by both humoral and cellular responses. Cytokines and chemokines such as CXCL12 and CCL21 regulate immune cells recruitment, metastasis [13,14] and angiogenesis [14,15] being key chemokines for EPCs recruitment and maturation [16,17]. The cell crosstalk operates by the modulation of adhesion molecules as selectins and chemokine receptors which interact with the extracellular matrix molecules such as podoplanin [18], mediating CCL21 presentation by cancer activated fibroblasts (Tejchman et al. Oncotarget, in press). This mechanism controls the tumour-cell movements thus metastatic escape [19,20] and immune cells recruitment in the tumour site [21].

It should be emphasized that such effects may result from the upstream dysregulation of the microRNAs (miRs), which are key gene modulators of the tumour microenvironment balance. The angiogenesis-controlling MiRs, angiomiRs and hypoxamiRs, are induced by tumour hypoxia and often promote pathologic vasculature; thus they constitute therapeutic targets [22]. Therefore, their role in tumour microenvironment is crucial and their pattern of expression is of potential diagnostic value. MiR expression can be highly characteristic as miR1246 overexpression in tumour endothelial cells [23].

Tumour angiogenesis takes advantage of the progenitor cells plasticity both endothelial and tumoural. Cancer stem-like cells (CSC) were described as mimicking microvascular endothelial cells and endothelial precursors cells in the tumour niches [24,25]. This suggests that tumour and endothelial cells interactions occur in hypoxia as inside tumour niches [26].

In this view, the place and conditions in which CSCs originate as well as their microenvironment remain controversial. CSCs were often observed associated with endothelial cells, thus the cancer stem cell niche was first understood as non-hypoxic although resistance to hypoxia is a characteristic feature of CSCs [5,27] and stemness phenotype is stabilized by hypoxia [28].

Acting through the production of factors able to exert a paracrine chemoattractant effect, CSCs may sensitize endothelial cells, especially progenitors ECs for recruitment into the tumour site [29].

Consequently, to study *in vitro* tumour reactivity, the very first step would be to reconstitute tumour angiogenesis utilizing tools able to mimic and respond to tumour signals. In the present melanoma tumour model, angiogenesis was achieved by endothelial progenitors to mimic tumour-recruited ECs while, in the approach of the metastatic process, lung-derived mature endothelial cells were used.

Hypoxic conditions are usually reproduced in classical 2D co-cultures, but the tumour is organized three-dimensionally. Spheroid structure allows *in vitro* the normal establishment of hypoxia along the spheroid structure development [30,31].

Taking the selected parameters into account, this work shows the new possibilities brought by a biologically relevant model for *in vitro* cancer studies. Focused on the angiogenic reaction under hypoxic conditions the 3D model demonstrates interactions of EEPCs with tumour-cells inside a 3D structure. The profound effects of hypoxia and tumour angiogenesis reconstruction were shown by changes in the humoral composition, especially in microRNA expression pattern evaluated in each distinct cell component of the tumour models.

Materials and methods

Details on cell lines, cell culture, co-cultures of melanoma with endothelial cells, fluorescent labelling of cells, cancer stem-like cells typing by ALDH activity, cloning for spheroid formation, *In vitro* pseudo tube formation, HIF-1α production and estimation, chemokines assessment by ELISA tests, extraction of cells from 3D tumour models for miRNA analysis, quantitative PCR and statistical analysis are described in Supplementary Materials and methods.

Spheroid formation

To obtain spheroids from B16-F10 and M10 lines, 1000 cells were mixed with a 0.25% (w/v) methylcellulose (R&D, HSC001) solution in culture medium (30 μL) and seeded in Perfecta3D® 96-Well Hanging Drop Plates (3D Biomatrix, HDP1096-8). After 48 h incubation at 37 °C in a 5% CO_2/95% air atmosphere, a single spheroid per drop was obtained.

3D cell model of melanoma microenvironment

The matrix is collagen type I (CORNING, #354236) 1.6 mg/mL PBS completed with FBS (10% v/v), 1.12% of methylcellulose w/v and Matrigel™ 25% (v/v). MAgECs 10.5, MAgECs 11.5 and Lung FVB cells were stained with Lipophilic Tracers – DiI, DiO and DiD respectively. 5×10^5 of each EC line was mixed with 50 spheroids inside of 225 μL of cold matrix and put in wells of a 24 well-plate. Control spheroids were fixed by 4% PFA in PBS (w/v) for 30 min and neutralized by 20 mM urea in PBS, for 30 min. Matrix polymerization at 37 °C was allowed for 1 h 250 μL of OptiMEM were poured gently. The plate was introduced into the incubation chamber of the video microscope station at 37 °C, 5% CO_2, and 18.75% O_2 (normoxia) or 1% O_2 (hypoxia). Time-lapse acquisitions were performed each hour over 24 h with a Zeiss Axiovert 200M fluorescence inverted microscope (Zeiss).

A human 3D model of melanoma was also prepared in a similar matrix. HEPC.CB1 cells stained with PKH67, HSkMEC cells stained with DiD and M10 melanoma spheroids were utilized. 5×10^5 of each EC line was mixed with 50 melanoma spheroids inside 225 μL of cold matrix in wells of a 24 well-plate.

3D models with ALDH positive or negative spheroids were prepared by mixing 20 B16F10 $ALDH^+$ or $ALDH^-$ spheroids (14 day-cultures after cloning) with 5×10^5 of DiI stained MAgECs 11.5 and DiO stained Lung FVB.

Images were analysed by "Image J" software. ECs migration was measured based on fluorescence. The integrated density of fluorescence from each channel (FITC for DiO and PKH67; DsRED for DiI and PKH26; Cy5 for DiD) was measured in the area occupied by the spheroids. Changes were expressed as a function of time. The data were normalized with reference to 100% integrated density value at t = 2 h.

Results

3D cell cultures by spheroid formation

Characterization of the melanoma cells ability to form spheroids

To build a 3D type of melanoma micro-tumour, a perfecta 3D system was used. Round, compact spheroids from murine (Fig. 1A) and human (Fig. 1B) melanoma cell lines from 1000 B16F10 and M10 were formed. After 48 h of culture, spheroids contained 1700 (+/− 200) cells. Cell organization inside spheroids was visualized by Apotome (Zeiss Axiovert 200M fluorescence microscope) as a cohesive layer of M10 cells (Fig. 1C). Moreover the intra spheroid cell motility was evidenced for M10 cells (Supplementary video S1).

Supplementary data related to this article can be found online at http://dx.doi.org/10.1016/j.canlet.2017.03.006.

HIF-1α stabilization by hypoxia in the 3D spheroids of melanoma

HIF-1α stabilization is an effect of hypoxia in cells. Hypoxia inside spheroids was studied and reported by ELISA assay for HIF-1α

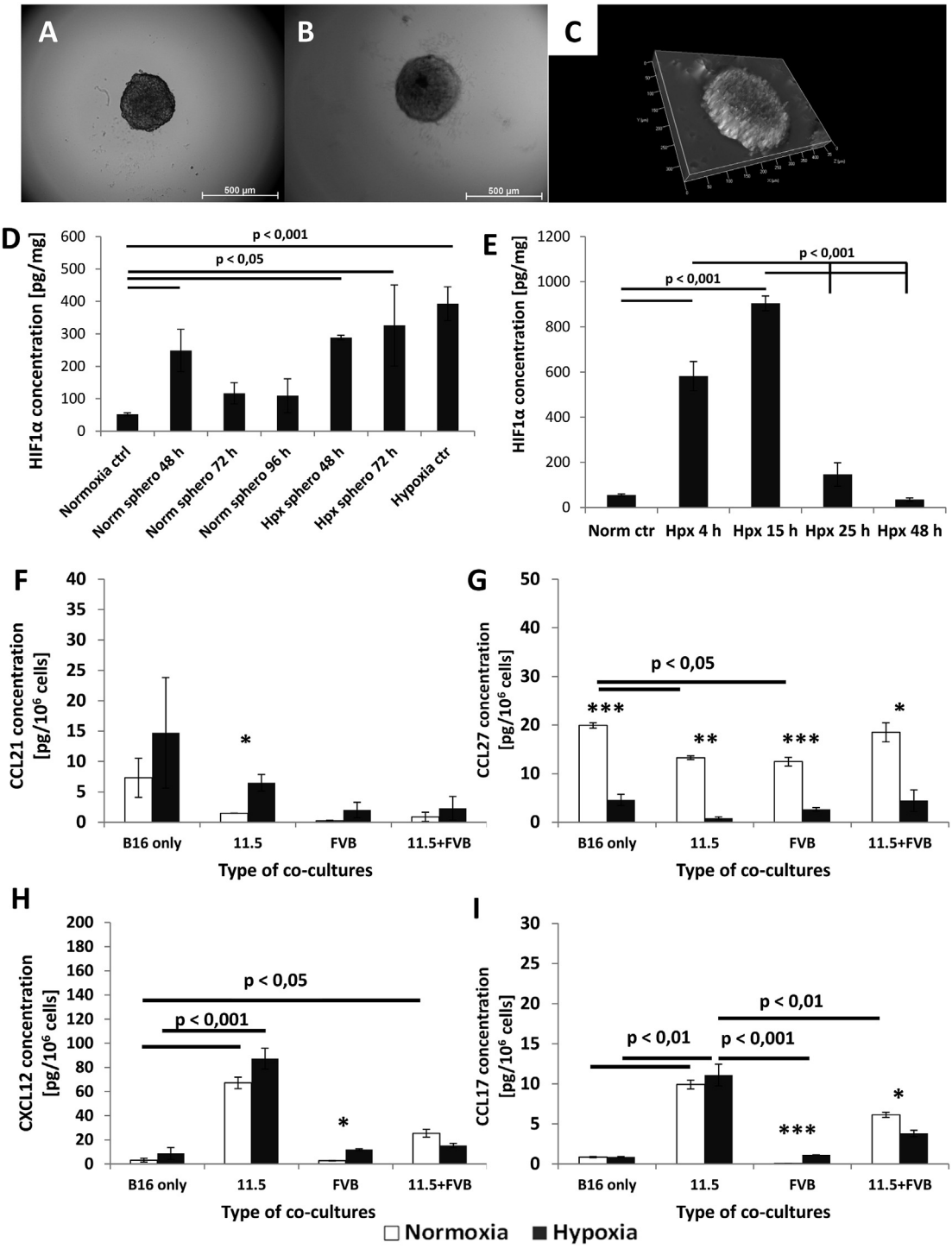

Fig. 1. Characterization of the 3-dimensional cell cultures of murine and human melanoma. Spheroids formed using Perfecta 3D system from 1000 cells of murine B16F10 (A) or human M10 (B) melanoma after 48 h of culture. (C) Image of the 35 µm slice of M10 melanoma spheroid. (D) Kinetics of HIF-1α production by B16F10 spheroids in normoxia and hypoxia. Mean +/− SEM. (E) Kinetics of HIF-1α production by B16F10 cell monolayers. Mean +/− SEM. (F–I) Chemokine production by co-cultures of B16F10 melanoma cells with mature and progenitor ECs. Normalized results of ELISA tests for CCL21 (F), CCL27 (G), CXCL12 (H), CCL17 (I). Mean +/− SEM. * − $p < 0.05$; ** − $p < 0.01$; *** − $p < 0.001$.

(Fig. 1D). In 48 h old spheroids the concentration of HIF-1α was similar in normoxia or hypoxia. For longer incubations in hypoxia, the HIF-1α concentration was stable. HIF-1α lowered in spheroids grown in normoxia after 48 h (Fig. 1D) as compared to 2D cell monolayers in hypoxia, where HIF-1α concentration increased then decreased (Fig. 1E).

Chemokines production by the co-cultured melanoma and endothelial cells, influence of hypoxia

Cell-to-cell crosstalk was investigated in co-cultures of melanoma cells and ECs under normoxia and hypoxia. Expressions of CCL21 (6CKine), CCL27 (CTACK), CXCL12 (SDF-1), CCL17 (TARC), and CX3CL1 (fractalkine) was measured. CCL21 expression reduced

upon co-culture of tumour cells with ECs. The hypoxia increased CCL21 production mainly with MAgEC11.5 EPC (Fig. 1F). Hypoxia effect on CCL27 was the opposite (Fig. 1G), consistently reducing production by tumour cells alone or with ECs for, either adult or progenitors. This effect was reversed in co-culture with both ECs. CXCL12 production was enhanced in B16F10 cells and EPCs co-cultures. The hypoxia effect was weak (Fig. 1H). CCL17 production was comparable to CXCL12, which is stimulated by co-culture with EPCs only (Fig. 1I) showing the distinct effects of EPC vs mature endothelial cells on the melanoma cells. No production of CX3CL1 was detected.

Stem like cancer cells selection and phenotype stabilization by hypoxia in spheroids

2D cultures of melanoma cells contained very low proportions of CSCs detectable by stemness markers. Fig. 2 shows that CD133 and CD271 are poorly expressed in the B16F10 cells (1% and 0, 5% respectively) while CD 44 and CD24 were expressed on the total cell population. None of these antigens was modulated by hypoxia (Fig. 2A). The influence of pO_2 was evidenced in B16F10 cells upon labelling for ALDH activity (Fig. 2B). The cell population expressing ALDH reached 18% upon treatment of the cells in hypoxia for 24 h (Fig. 2C). ALDH activation was pO_2-sensitive (Fig. 2D) and plateaued after 12 h, in $pO_2 \leq 5\%$ (Fig. 2C). Hypoxia stabilized the stem-like phenotype (Fig. 2E and F) where the ALDH+ subpopulation counted for around 15% after 72 h in hypoxia (Fig. 2E). Upon sorting and keeping the hypoxic conditions the population remained ALDH+ after 2 weeks in culture (Fig. 2F).

B16F10 cells, sorted for ALDH activity, were used to prepare spheroids either from 60 sorted tumour cells (Fig. 2G–O) or from one cloned B16 F10 (Fig. 2P). $ALDH^-$ spheroids grew faster (Fig. 2G and K) and formed easier than $ALDH^+$ spheroids (Fig. 2O and P). However when stromal cells, like EPCs (Fig. 2H and L) or fibroblasts (Fig. 2I and M), were seeded with tumour cells this effect was reversed. Less spheroids grew from $ALDH^-$ cells in the presence of endothelial progenitors or/and fibroblasts (Fig. 2O and P). The reduction of $ALDH^-$ spheroid growth and increase of ALDH+ spheroid growth were confirmed when both stromal cells were added (Fig. 2J and N) as shown by the yield of spheroid formation (Fig. 2O and P).

Characterization of angiogenic properties of selected mature and progenitor ECs

The formation of pseudo-vessels by murine progenitor and mature ECs was performed in 2D Matrigel (Fig. 3A–C) as mixed angiogenesis involving EC lines in pairs (Fig. 3D–F) and all together (Fig. 3G). The same experiments were performed with human progenitor and mature EC lines (Fig. 3H–N). Images are from t = 5H. Quantitative analysis of the networks was done using an Angiogenesis Analyser macro (from Gilles Carpentier Research) for ImageJ graphic software and presented on graphs (Fig. 3O–V). Murine EPCs alone did not form pseudo-vessels as opposed to the numerous, short pseudo-vessels with loops from mature ECs (Fig. 3A–C, O–R). However EPCs cooperate to form longer but less pseudo-vessels, than other ECs mixes (Fig. 3F, O–R). Pseudo-vessel networks were efficiently formed by mixed progenitors and mature ECs (Fig. 3G). These data were confirmed by angiogenesis achieved by human endothelial progenitor and mature cells (Fig. 3H–N and S–V). HEPC.CB1 and HEPC.CB2 alone did not form pseudo vessels but both progenitors cells cooperate to vessel formation (Fig. 3M, S–V). Both progenitor cells cooperated with the mature HSkMECs to produce vessels (Fig. 3K–N). Supplementary video S2 shows that all EC types cooperated to create stable pseudo-vessels as compared to individual cell as shown for HSkMECs (Fig. 3N, S–V, and supplementary video S3).

Supplementary data related to this article can be found online at http://dx.doi.org/10.1016/j.canlet.2017.03.006.

3D model of melanoma microenvironment: ability to recruit angiogenic endothelial cells and endothelial progenitor cells

To reproduce tumour microenvironment, 3D models of tumour were composed of murine B16F10 melanoma spheroids which were placed in the presence of mature and progenitor murine ECs in collagen/matrigel matrix (Fig. 4A–F).

ECs migrated toward living B16F10-spheroids in hypoxia (Fig. 4A and B) and normoxia (Fig. 4D and E) as opposed to fixed B16F10-spheroids (Fig. 4C and F). As quantified previously [31] and displayed here (Fig. 4A–F), ECs recruitment by melanoma spheroids was higher in hypoxia (Fig. 4B) than in normoxia which displayed disorganized ECs migration (Fig. 4E). Early endothelial precursor cell (MAgEC10.5) recruitment was 5 fold higher in hypoxia than in normoxia while it was twice increased for more mature ECs (MAgEC11.5 and Lung FVB ECs).

ECs migration was also observed in the human 3D model of melanoma microenvironment (Fig. 4G–N) in hypoxia compared to normoxia. Confirming the murine models data [31], human ECs recruitment was similarly visible only in tumour models containing living melanoma spheroids (Fig. 4G–I, K–M) while no recruitment occurred in tumour models with fixed cells-containing spheroids (Fig. 4J and N). Low oxygen tension not only increased ECs migration toward spheroid (Fig. 4G–I), but also promoted ECs' organization in a web-like network surrounding the melanoma spheroid as visible after 24 h (Fig. 4H and supplementary video S4). When the models were allowed to develop over 6 days, hypoxia-mediated recruitment of ECs increased greatly (Fig. 4I and Supplementary Figure S1). In normoxia, the previously non-organized recruitment of ECs (Fig. 4L) evolved in the long term, into a complex network with cord-like structures surrounding melanoma spheroid (Fig. 4M and Supplementary Figure S2) suggesting that hypoxia appeared in the long-term developing spheroids.

Supplementary data related to this article can be found online at http://dx.doi.org/10.1016/j.canlet.2017.03.006.

The murine 3D model of melanoma microenvironment was further utilized to identify the tumour cell population responsible for ECs recruitment and test the CSCs ability to specifically recruit EPCs. We compared tumour-spheroids consisting of stem-like $ALDH^+$ (Fig. 4O–Q) to $ALDH^-$ cells (Fig. 4R–T) in progenitors recruitment compared to mature ECs. Quantification is reported on Fig. 5(A–D).

Recruitment of each EC type by melanoma spheroids in 3D tumour models could be quantified by ECs fluorescence co-localization with spheroids. A demonstration that hypoxia specifically increases EPCs recruitment by tumours [31] was extended to the human tumour model (Fig. 5A and B). Moreover, the recruitment of mature human ECs, decreased in low oxygen tension (Fig. 5B). Quantification performed for murine 3D tumour models containing $ALDH^+$ or $ALDH^-$ melanoma cells (Fig. 5C and D) showed a great specificity in EPCs recruitment by ALDH+ spheroids as opposed to $ALDH^-$ spheroids and compared to mature ECs which did not display any selectivity.

3D model of melanoma microenvironment: analysis of melanoma-to-EC intercellular interactions

Melanoma spheroids and recruited ECs were extracted from the matrix. Cell suspensions obtained from the murine tumour models were analysed by flow cytometry for their fluorescence characteristics (Fig. 5E–H). Cells dispersed from spheroids in hypoxia evidenced the exchange of dye since some cell

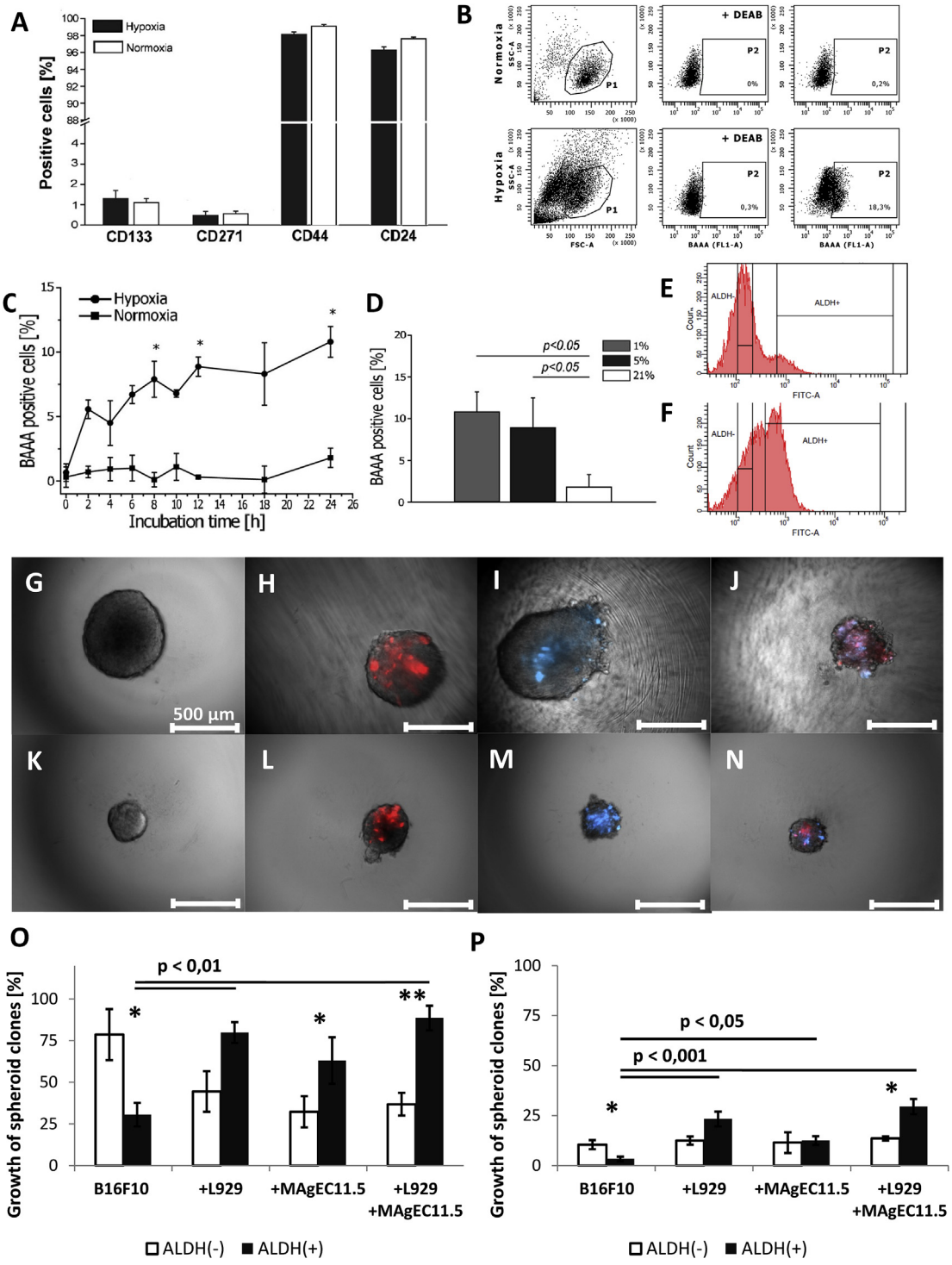

Fig. 2. Stem like cancer cells selection and phenotype stabilization by hypoxia in spheroids. (**A**) CD24, CD44, CD133 and CD271 on B16F10 cells in normoxia and hypoxia. Mean ± SE; N = 3. (**B**) Hypoxia activation of ALDH in B16F10 cells assessed by flow cytometry. Gated living cells (P1) with ALDEFLUOR (BAAA) displayed ALDH activity in hypoxia (P2). Control level is given in the presence of DEAB inhibitor of ALDH. (**C**) Kinetics of ALDH activation as % of BAAA positive cells in normoxia and hypoxia, over 24 h as means ± SE; N = 3; * – $p < 0.05$. (**D**) B16F10 cells were cultured for 12 h under $pO_2 = 1\%$, 5% and 21%; mean ± SE; N = 3; * – $p < 0.05$. (**E**) B16F10 cells incubated 72 h in hypoxia and flow cytometry analysed for ALDH activity. (**F**) Flow cytometry analysis of sorted $ALDH^+$ cells cultured in hypoxia for 2 weeks. (**G–N**) Spheroids formed from ALDH negative 60 sorted cells per well of V-shaped non-adherent 96-well plate (**G–J**) or from ALDH positive cells (**K–N**). MAgECs 11.5 (**H, L**), fibroblasts L929 (**I, M**) or both (**J, N**) were added in equal proportions keeping equal final number of sorted cells per well. Images were captured after 2 weeks, with 5× objective. (**O, P**) Yield of spheroid formation from sorted B16F10 cells. (**O**) 60 sorted cells per well and (**P**) 1 sorted cell per well. Mean +/− SEM. Values significantly different between $ALDH^-$ and $ALDH^+$ spheroids were marked with: * – $p < 0.05$; ** – $p < 0.01$; *** – $p < 0.001$.

populations were carrying more than one dye (Fig. 5E). This specifically occurred in hypoxia as, in normoxia-maintained spheroids, the fluorescence of each cell population remained distinct (Fig. 5F). Tumour-to-ECs interactions were evidenced by the dye-exchange from ECs to non-labelled B16F10 melanoma cells that acquired fluorescence properties when extracted from 4-days tumour models (Fig. 5E–H). In hypoxia most of B16F10 cells acquired fluorescence mainly from MAgEC 10.5 and MAgEC 11.5 cells

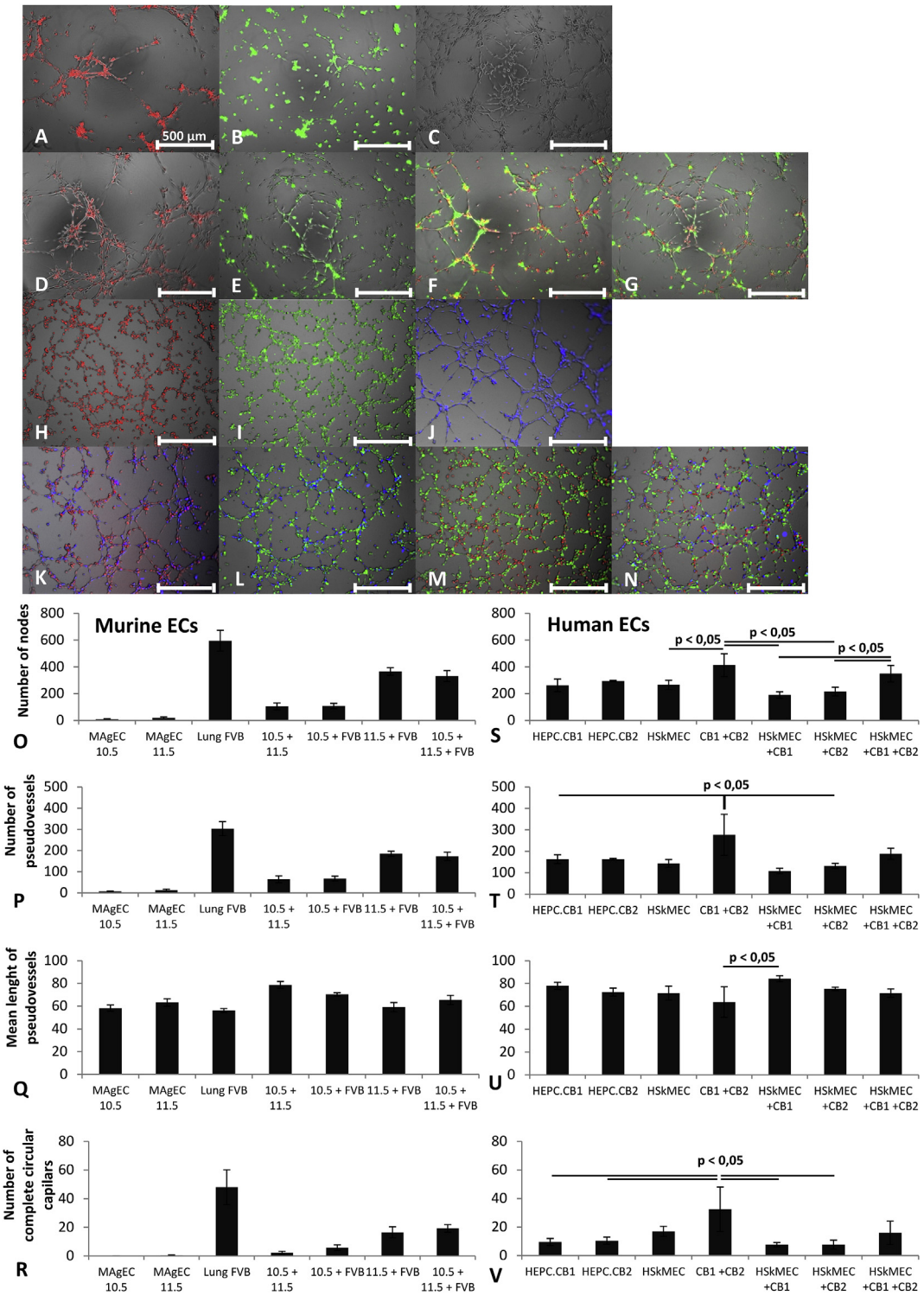

Fig. 3. Estimation of angiogenic properties and cooperation of mature and progenitor ECs. (A–G) 2D angiogenesis assay for murine ECs alone (A–C), in pairs (D–F) and, all together (G) – MagEC 10.5 (red), MAgEC 11.5 (green), Lung FVB (not stained). (H–N) Similar angiogenesis assays for human ECs alone (H–J), in pairs (K–M) and together (N). HEPC. CB1 (red), HEPC.CB2 (green), HSkMEC (blue). Pictures represent t = 5H. (O–V) Quantitative analysis of angiogenesis performed by murine (O–R) and human (S–V) ECs. Number of nodes (O, S), pseudo-vessels (P, T), mean length of pseudo-vessels (Q, U) and complete circular capillaries (R, V) were quantified at t = 5H. Mean +/− SEM. Statistical analysis was performed using ANOVA analysis and post-hoc Tukey test (HSD).

(Fig. 5E and G). In normoxia, no interaction occurred with MAgEC10.5 or 11.5, showing the specificity of the hypoxia-induced interactions of tumour cells with early endothelial progenitors, because in normoxic conditions, dye transfer only occurred with mature endothelial cells (Fig. 5F and H).

3D model of melanoma microenvironment: characterization of the of microRNAs expression profile

MicroRNAs expression was measured in the whole tumour model cell populations i.e. B16F10 melanoma and recruited endothelial cells. Hypoxic conditions were compared to normoxia

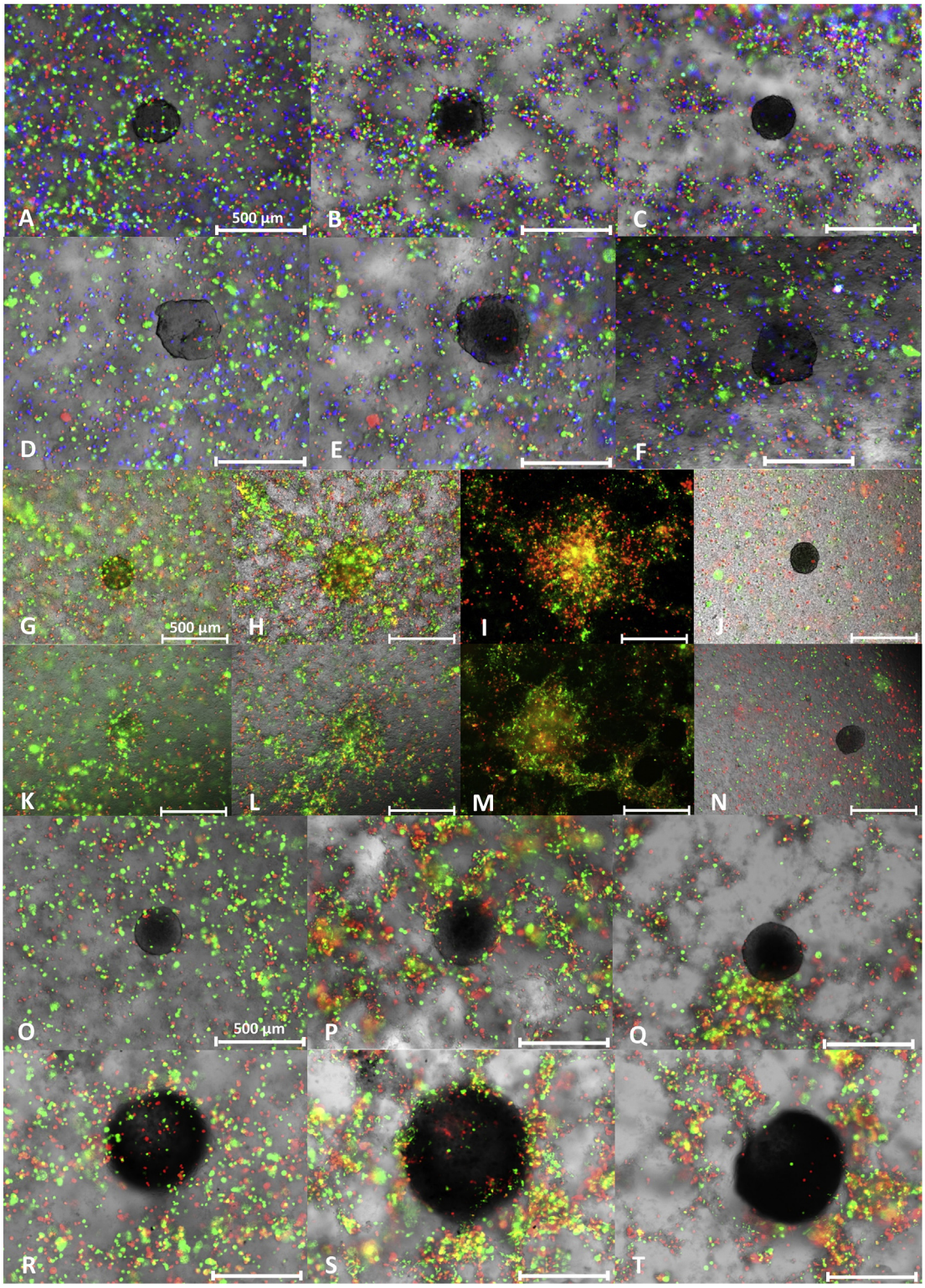

Fig. 4. Recruitment of ECs by melanoma spheroids inside 3D cell model of melanoma micro-environment. (A–F) Recruitment of MAgECs 10.5 (red), MAgECs 11.5 (green) and Lung FVB (blue) cells by B16F10 melanoma spheroids in hypoxia (A–C) and normoxia (D–F) after 2 h (A, D) and 24 h (B, E). 3D tumour models with fixed spheroids as negative control at t = 24H (C, F). (G–N) Recruitment of HEPC.CB1 (green) and HSkMEC (red) cells by M10 melanoma spheroids in hypoxia (G–J) and normoxia (K–N) after 2 h (G, K), 24 h (H, L) and 6 days (I, M). 3D tumour models with fixed spheroids as negative control at t = 24H (J, N). (O–T) Recruitment of MAgECs 11.5 (red) and Lung FVB cells (green) by B16F10 ALDH$^+$ (O–Q) and ALDH$^-$ (R–T) spheroids in hypoxia after 2 h (O, R) and 24 h (P, S). 3D tumour models with fixed spheroids as negative control at t = 24H (Q, T).

(Fig. 6A) and data validated living spheroids activity (Fig. 6B). Hypoxia slightly increased the expression of miR-126 and 210-3p, significantly upregulated miR-21 and greatly increased the production of miR-1246 (Fig. 6A). Hypoxia decreased the expression of miR-29b compared to normoxia. MiR-21 and 1246 increased in living spheroid models (Fig. 6B). MicroRNAs expression was also measured in cells from tumour model after fluorescence-based cell sorting of each line (Fig. 6C–F).

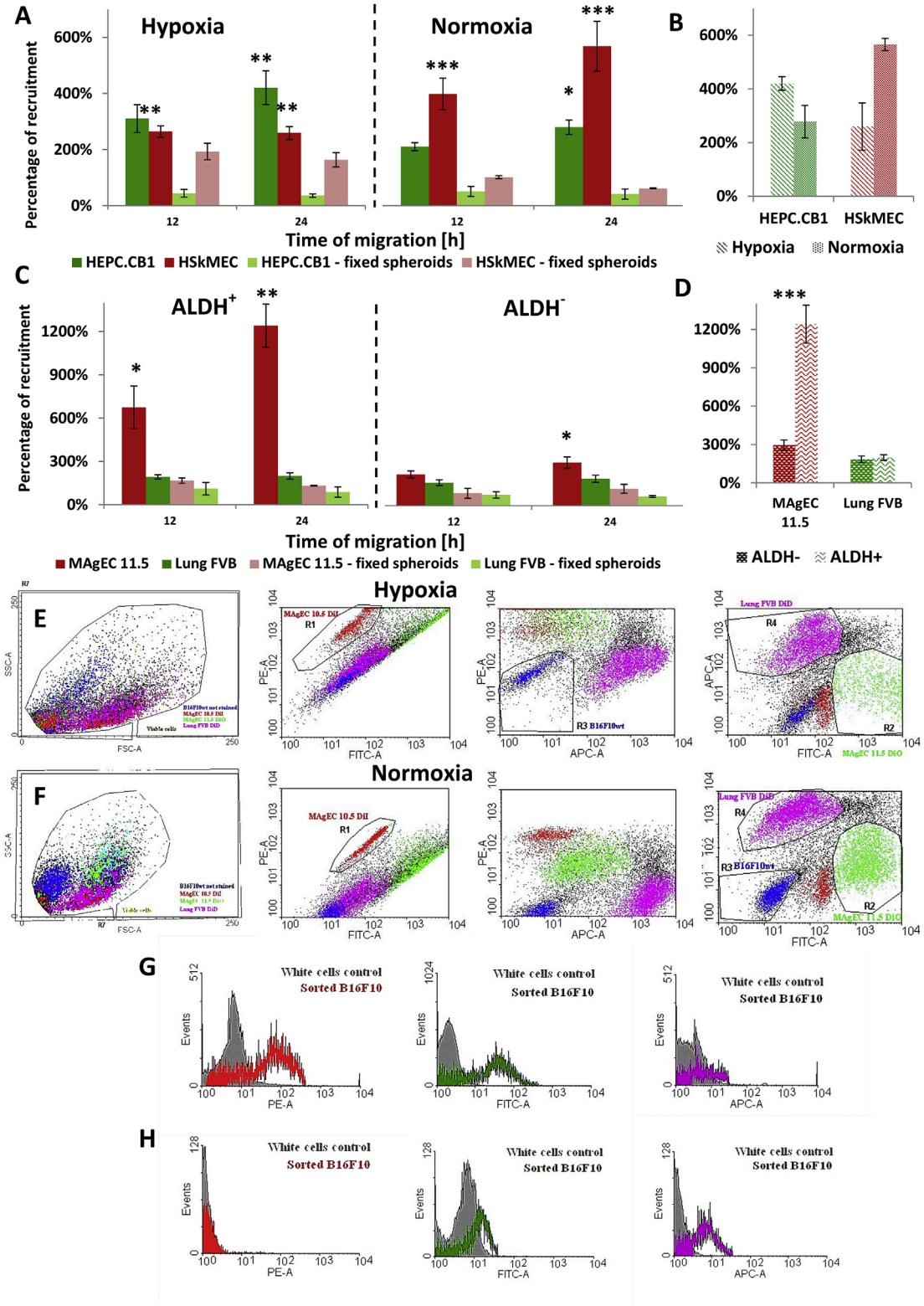

Fig. 5. Quantification of ECs recruitment in 3D models of melanoma micro-environment and flow cytometry analysis of extracted cells. (A) Recruitment of ECs in human 3D model of melanoma in hypoxia and normoxia. (B) Effect of hypoxia on ECs recruitment after 24 H. (C) Recruitment of ECs in murine 3D model of tumour containing normal or stem-like melanoma spheroids in hypoxia. (D) ECs recruitment compared between $ALDH^+$ and $ALDH^-$ spheroids. Mean +/− SEM. Values statistically significantly different from T = 2 h (A, C), between hypoxia and normoxia (B) or $ALDH^+$ and $ALDH^-$ (D) were marked with: * − $p < 0{,}05$; ** − $p < 0{,}01$; *** − $p < 0{,}001$. (E–H) Flow cytometry analysis of ECs extracted from murine 3D model of tumour incubated for 4 days in hypoxia (E) or normoxia (F). Interaction between B16F10 melanoma cells and ECs was estimated based on dye exchange in hypoxia (G) and normoxia (H).

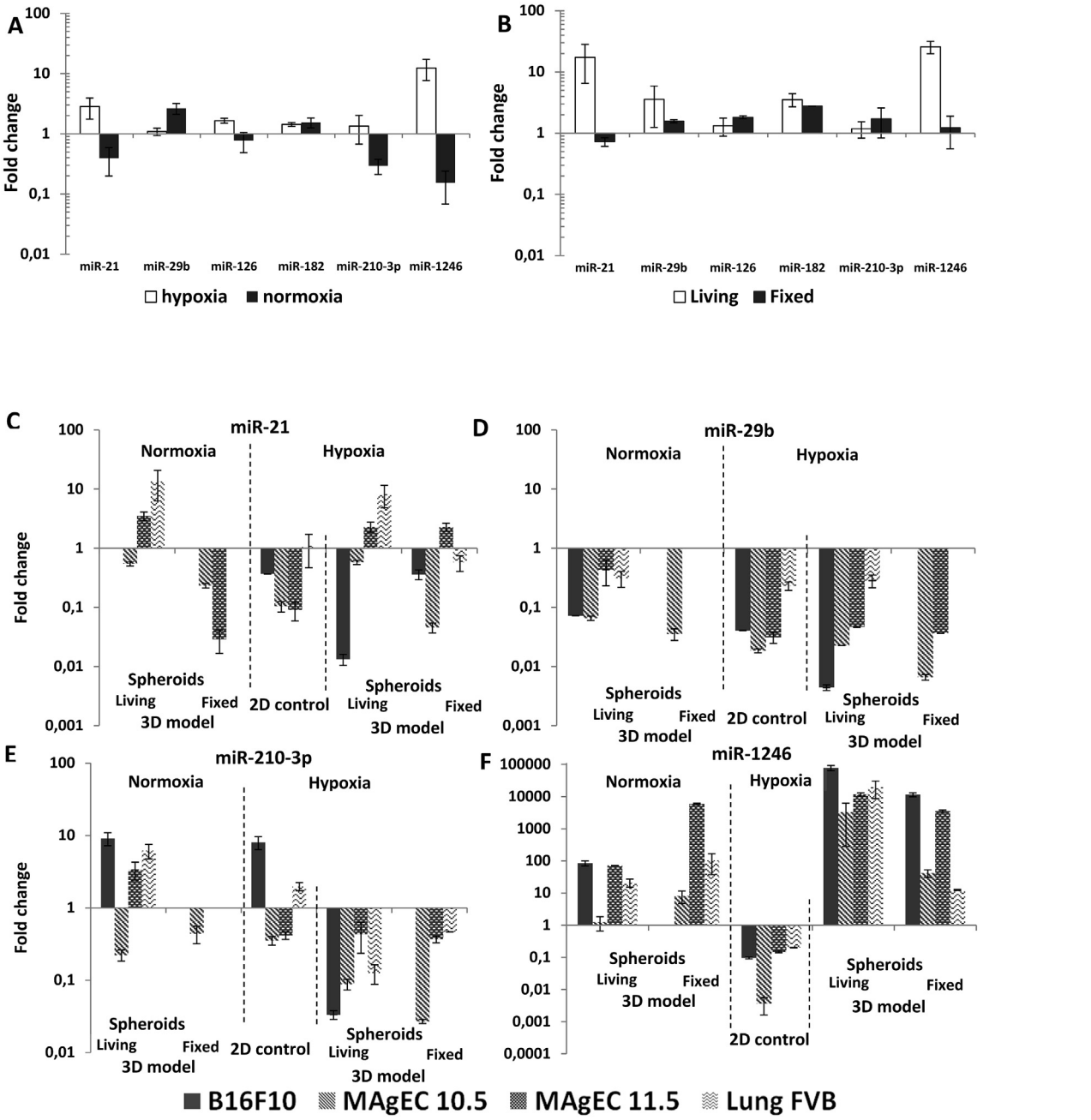

Fig. 6. microRNA expression in cells extracted from murine 3D model of melanoma micro-environment. (A, B) AngiomiRs expression in extracted mixture of B16F10 and recruited ECs from tumour model. (A) Effect of hypoxia on miRs production. (B) Comparison of miRs expression between tumour model with living and fixed melanoma spheroids. (C–F) Cells extracted from spheroids were sorted into separate melanoma and endothelial cell lines. Production of miR-21 (C), miR-29b (D), miR-210-3p (E) and miR-1246 was measured in comparison to 2D cell cultures in normoxia.

MiR-21 was efficiently upregulated in 3D models, similarly in hypoxia and normoxia and this effect concerned the MAgEC11.5 EPCs and mature Lung FVB ECs (Fig. 6C). The production of miR-29b was always lower in cells from tumour models and monolayers in hypoxia than in cells from controls in normoxia. Downregulation was observed in the tumour model in normoxia but enhanced by hypoxia in 3D and 2D culture conditions (Fig. 6D). MiR-210 expression was upregulated in hypoxia only for B16F10 and endothelial lung FVB cells in 2D cultures (Fig. 6E). In tumour models miR-210 production was increased only in normoxia (B16F10, MAgEC 11.5 and lung FVB) and decreased in all cells in hypoxia (Fig. 6E). The expression of miR-1246 greatly increased in normoxia, in all cells of the tumour model, excluding MAgECs 10.5. MiR-1246 expression was elevated 1000 times by hypoxia in all cells from tumour model (Fig. 6F) while it was down regulated in cell lines cultured in 2D in hypoxia.

Discussion

This work shows the advantage of 3D tumour models with properly defined microenvironment to mimic the tumour development *in vivo*. To-date methods provide only partial information about tumour development for their inherent limitations in facilitating access to variables and parameters relevant of *in vivo*

conditions. Consequently, alternative cell culture methods which permit to get closer to these conditions mimicking 3D growth, proper oxygen tension, and stromal-to-tumour cell interactions and communications in tumour microenvironment are of critical need for cancer research. When a solid tumour develops, the first step of the stroma establishment occurs with the involvement of the endothelial cells that are prompted to form vessels by the angiogenic switch upon hypoxia establishment in the tumour mass [32]. The aim was to determine the conditions for a 3D cellular model that would allow investigating the mechanisms of tumour vascularization taking into account the local vessel sprouting [4] and elucidating the role of EPCs [31] in pathologic tumour angiogenesis [33].

The differential role played by mature and progenitor ECs were shown in vessel formation and in the interactions with tumour cells. Indeed, cells from a mature endothelial cell line [34] built vessel-like tubes whereas MAgECs, representative of endothelial progenitors [31], incorporated into neovessels helping the formation of pathologic tumour angiogenesis.

This effect was confirmed in a human model showing the active cooperation between human mature and progenitor endothelial cells [35,36] to form stable and organized pseudo-vessel network.

The angiogenic switch is the signal for tumour stroma development; therefore the effect of a low oxygen tension on modulating the process of tumour vascularization was examined in this 3D model. The model proved its value to study tumour specific recruitment signals. Indeed, it enabled us to demonstrate the specific recruitment of early endothelial progenitor cells (EEPCs) by the tumour. Moreover, the tumour deep hypoxia was shown to be a selective pressure for the cancer stem-like cell phenotype. We have demonstrated that this cell population can be characterized in the melanoma, by an increased activity of the aldehyde dehydrogenase − ALDH [37]. These ALDH+ cells are hypoxia-selected and stabilized. In the 3D tumour model, they selectively recruit EEPCs. This process is specific for only CSCs and hypoxia. Indeed, $ALDH^{-}$ cell spheroids did not recruit EEPCs efficiently even in hypoxia. As CSCs are the main targets to be reached in cancer treatment [38,39], the demonstration that endothelial precursors of defined phenotype are actively attracted into the tumour site by CSCs enhances the perspectives of new treatment opportunities and of cell-gene therapy based on EEPC-mediated tumour targeting [31]. Flow cytometry analyses confirmed that, in hypoxia only, EEPCs interacted closely enough with tumour cells to enable the transfer of lipophilic fluorescent dyes. Hypoxia-selective recruitment was also shown using the human 3D model of melanoma, where low oxygen tension not only increased EPCs recruitment, but also hindered the recruitment of mature ECs. Thus, the 3D spheroid model of tumour distinguished the cell mechanism of early endothelial precursor cell recruitment in the tumour by CSCs showing its potential for future cellular and molecular information on the cancer microenvironment-mediated effects. The stromal composition was completed by the addition of fibroblasts which played a fundamental role in helping tumour growth. Not only endothelial progenitors, but also fibroblasts, are important in the creation of a stable tumour-stem-like cell niche. CSCs and endothelial precursor cells are cooperating closely in the vascular/cancer stem niche. Cell-to-cell cross-talk operates through chemokines such as CCL17, CCL21, CCL27, and CXCL12, regulating EPCs migration and tumour cells escape. Similarly, microRNAs mediate the EC-to-CSCs cross-talk, because they act on cells by regulating gene expression. Hypoxa-miRs, induced under hypoxia, act on angiogenesis either directly or by action on angiomiRs [33]. In tumours, miR-210, is HIF-1α-dependent and helps its stabilization, thus controlling the hypoxic phenotype. The designed 3D tumour model established both HIF-1α and miR-210 production under normoxic external conditions, corroborating the setting of hypoxia inside such 3D structures [40,41] and their stabilization under prolonged hypoxic external conditions [40]. Among other hypoxa-miRs and angiomiRs miR-21 which induces angiogenesis through AKT activation and targets PTEN [42], is increased in ECs in hypoxia growing spheroids. MiR-29b which has many effects on cancer evolution working as a tumour suppressor [43], consistently decreased in all cell populations in spheroids and in response to hypoxia. MiR-1246, which controls angiogenesis in cancer [23], increased in all cells of the 3D tumour model especially in hypoxia as opposed to its decrease in 2D cultured cells. Thus, our data point to the importance of utilizing cell culture methods that provide access to the tumour microenvironment. Indeed, in standard 2D cultures in hypoxia the expression of miR-21 and miR-1246 decreased compared to the control in normoxia, and the expression of the miR-21 was highly elevated in the 3D tumour model, and this effect was considerably greater for the miR-1246 expression in all cell populations that composed the tumour 3D models. Thus, although 2D cultures showed that hypoxia influences the cell response by the modulation of miR expression, the use of tridimensional tumour models, in which the cellular and molecular components that contribute to the tumour tissue development, are taken into account, appears of fundamental importance. The miR response illustrates this effect, as it appears in the 3D models to be different or even opposite to the response obtained in 2D. This response in 3D conditions is in agreement with *in vivo* reported data. The designed 3D tumour models make it possible to study, *in vitro*, the fine-tuning of the microenvironment processes like tumour-angiogenesis. It underlines the key role of tumour hypoxia in the selection of tumour stem cells and their action in specifically recruiting early endothelial progenitors. Our observations point clearly to the weakness of classical 2D cell culture methods in normoxia and the risk of providing biologically irrelevant data. They provide a new means to approach the mechanism of vessels formation in tumours and to evidence interactions inside the tumour site. Despite limitations inherent to *in vitro* simplifications, the designed 3D spheroid tumour model makes a step forward in the reconstitution of tumour pathology.

Acknowledgements

We thank, David Gosset of P@CYFIC platform facility in the Center for Molecular Biophysics for the help in flow cytometry technique and for cell sorting.

Krzysztof Klimkiewicz was a doctoral fellow sponsored by the French Embassy fellowship and Campus France for doctoral studies in the frame of the French Polish co tutorial doctoral program and the doctoral program of the Jagiellonian University. Guillaume Collet was a doctoral fellow sponsored by the French Ministry of Research; fellowship No. 32852-2008, the Malopolska Marshal Office and the LNCC (National League Against Cancer).

This work was partly supported by the French-Polish Grant INCa/CNRS/MNiSW(347/N-INCA/2008) for cooperation and ANR "triple sens project", the LNCC, the Institut National de la Sante et de la Recherche Medicale (INSERM), the FEDER MiRPeau 5788/39114; the Harmonia Project No. 2012/06/M/NZ1/00008 supported by the National Science Center and "La Ligue Regionale contre le Cancer", the EU Framework Programs POIG 02.01.00-12-064/08 and 02.02.00- 00-014/08 and the STRATEGMED1/233574/14/NCBR/2015 grant ("Eptheron") Faculty of Biochemistry, Biophysics and Biotechnology of Jagiellonian University is a partner of the Leading National Research Center (KNOW) supported by the Ministry of Science and Higher Education. Research has been conducted in the scope of the MiR-TANGo International Associated Laboratory (LIA) and partly supported by the RCVL grant AIR MiRTAnGO.

Conflict of interest

Authors declare no conflict of interest.

Appendix A. Supplementary data

Supplementary data related to this article can be found at http://dx.doi.org/10.1016/j.canlet.2017.03.006.

References

[1] A. Santiago-Walker, L. Li, N.K. Haass, M. Herlyn, Melanocytes: from morphology to application, Skin. Pharmacol. Physiol. 22 (2009) 114–121.
[2] C. Perlis, M. Herlyn, Recent advances in melanoma biology, Oncologist 9 (2004) 182–187.
[3] J. Villanueva, M. Herlyn, Melanoma and the tumor microenvironment, Curr. Oncol. Rep. 10 (2008) 439–446.
[4] K.S. Smalley, M. Lioni, K. Noma, N.K. Haass, M. Herlyn, In vitro three-dimensional tumor microenvironment models for anticancer drug discovery, Expert Opin. Drug Discov. 3 (2008) 1–10.
[5] G. Collet, K. Skrzypek, C. Grillon, A. Matejuk, B. El Hafni-Rahbi, N. Lamerant-Fayel, et al., Hypoxia control to normalize pathologic angiogenesis: potential role for endothelial precursor cells and miRNAs regulation, Vasc. Pharmacol. 56 (2012) 252–261.
[6] K. Szade, M. Zukowska, A. Szade, G. Collet, D. Kloska, C. Kieda, et al., Spheroid-plug model as a tool to study tumor development, angiogenesis, and heterogeneity in vivo, Tumour Biol. J. Int. Soc. Oncodevelopmental Biol. Med. 37 (2016) 2481–2496.
[7] S. Chouaib, C. Kieda, H. Benlalam, M.Z. Noman, F. Mami-Chouaib, C. Ruegg, Endothelial cells as key determinants of the tumor microenvironment: interaction with tumor cells, extracellular matrix and immune killer cells, Crit. Rev. Immunol. 30 (2010) 529–545.
[8] B.A. Peters, L.A. Diaz, K. Polyak, L. Meszler, K. Romans, E.C. Guinan, et al., Contribution of bone marrow-derived endothelial cells to human tumor vasculature, Nat. Med. 11 (2005) 261–262.
[9] M. Franco, P. Roswall, E. Cortez, D. Hanahan, K. Pietras, Pericytes promote endothelial cell survival through induction of autocrine VEGF-A signaling and Bcl-w expression, Blood 118 (2011) 2906–2917.
[10] S. Goel, D.G. Duda, L. Xu, L.L. Munn, Y. Boucher, D. Fukumura, et al., Normalization of the vasculature for treatment of cancer and other diseases, Physiol. Rev. 91 (2011) 1071–1121.
[11] D. Hanahan, R.A. Weinberg, The hallmarks of cancer, Cell 100 (2000) 57–70.
[12] S. Goel, D. Fukumura, R.K. Jain, Normalization of the tumor vasculature through oncogenic inhibition: an emerging paradigm in tumor biology, Proc. Natl. Acad. Sci. U. S. A. 109 (2012) E1214.
[13] T. Barbai, Z. Fejos, L.G. Puskas, J. Timar, E. Raso, The importance of microenvironment: the role of CCL8 in metastasis formation of melanoma, Oncotarget 6 (2015) 29111–29128.
[14] H. Takeuchi, A. Fujimoto, M. Tanaka, T. Yamano, E. Hsueh, D.S. Hoon, CCL21 chemokine regulates chemokine receptor CCR7 bearing malignant melanoma cells, Clin. Cancer. Res. 10 (2004) 2351–2358.
[15] P. Tsui, A. Das, B. Whitaker, M. Tornetta, N. Stowell, P. Kesavan, et al., Generation, characterization and biological activity of CCL2 (MCP-1/JE) and CCL12 (MCP-5) specific antibodies, Hum. Antibodies 16 (2007) 117–125.
[16] S.R. Pickens, N.D. Chamberlain, M.V. Volin, R.M. Pope, N.E. Talarico, A.M. Mandelin 2nd, et al., Role of the CCL21 and CCR7 pathways in rheumatoid arthritis angiogenesis, Arthritis Rheum. 64 (2012) 2471–2481.
[17] P.V. Peplow, Influence of growth factors and cytokines on angiogenic function of endothelial progenitor cells: a review of in vitro human studies, Growth Factors 32 (2014) 83–116.
[18] M. Ugorski, P. Dziegiel, J. Suchanski, Podoplanin – a small glycoprotein with many faces, Am. J. Cancer Res. 6 (2016) 370–386.
[19] N. Eiro, F.J. Vizoso, Inflammation and cancer, World J. Gastrointest. Surg. 4 (2012) 62–72.
[20] A. Hoeben, B. Landuyt, M.S. Highley, H. Wildiers, A.T. Van Oosterom, E.A. De Bruijn, Vascular endothelial growth factor and angiogenesis, Pharmacol. Rev. 56 (2004) 549–580.
[21] D. Raman, P.J. Baugher, Y.M. Thu, A. Richmond, Role of chemokines in tumor growth, Cancer Lett. 256 (2007) 137–165.
[22] A. Matejuk, G. Collet, M. Nadim, C. Grillon, C. Kieda, MicroRNAs and tumor vasculature normalization: impact on anti-tumor immune response, Arch. Immunol. Ther. Exp. 61 (2013) 285–299.
[23] N. Yamada, N. Tsujimura, M. Kumazaki, H. Shinohara, K. Taniguchi, Y. Nakagawa, et al., Colorectal cancer cell-derived microvesicles containing microRNA-1246 promote angiogenesis by activating Smad 1/5/8 signaling elicited by PML down-regulation in endothelial cells, Biochim. Biophys. Acta 1839 (2014) 1256–1272.
[24] O. Shakhova, L. Sommer, Testing the cancer stem cell hypothesis in melanoma: the clinics will tell, Cancer Lett. 338 (2013) 74–81.
[25] G. Collet, B. El Hafny-Rahbi, M. Nadim, A. Tejchman, K. Klimkiewicz, C. Kieda, Hypoxia-shaped vascular niche for cancer stem cells, Contemp. Oncol. 19 (2015) A39–A43.
[26] Y.F. Ping, X. Zhang, X.W. Bian, Cancer stem cells and their vascular niche: do they benefit from each other? Cancer Lett. 380 (2016) 561–567.
[27] T. Borovski, E.M.F. De Sousa, L. Vermeulen, J.P. Medema, Cancer stem cell niche: the place to be, Cancer Res. 71 (2011) 634–639.
[28] C. Gorgun, S. Ozturk, S. Gokalp, S. Vatansever, S.I. Gurhan, A.S. Urkmez, Synergistic role of three dimensional niche and hypoxia on conservation of cancer stem cell phenotype, Int. J. Biol. Macromol. 90 (2016) 20–26.
[29] A. Filatova, T. Acker, B.K. Garvalov, The cancer stem cell niche(s): the crosstalk between glioma stem cells and their microenvironment, Biochim. Biophys. Acta 1830 (2013) 2496–2508.
[30] X. Xu, M.C. Farach-Carson, X. Jia, Three-dimensional in vitro tumor models for cancer research and drug evaluation, Biotechnol. Adv. 32 (2014) 1256–1268.
[31] G. Collet, K. Szade, W. Nowak, K. Klimkiewicz, B. El Hafny-Rahbi, K. Szczepanek, et al., Endothelial precursor cell-based therapy to target the pathologic angiogenesis and compensate tumor hypoxia, Cancer Lett. 370 (2016) 345–357.
[32] T. Hashimoto, F. Shibasaki, Hypoxia-inducible factor as an angiogenic master switch, Front. Pediatr. 3 (2015) 33.
[33] G. Collet, C. Grillon, M. Nadim, C. Kieda, Trojan horse at cellular level for tumor gene therapies, Gene 525 (2013) 208–216.
[34] N. Bizouarne, M. Mitterrand, M. Monsigny, C. Kieda, Characterization of membrane sugar-specific receptors in cultured high endothelial cells from mouse peripheral lymph nodes, Biol. Cell 79 (1993) 27–35.
[35] M. Paprocka, A. Krawczenko, D. Dus, A. Kantor, A. Carreau, C. Grillon, et al., CD133 positive progenitor endothelial cell lines from human cord blood, Cytom. Part A J. Int. Soc. Anal. Cytol. 79 (2011) 594–602.
[36] C. Kieda, M. Paprocka, A. Krawczenko, P. Zalecki, P. Dupuis, M. Monsigny, et al., New human microvascular endothelial cell lines with specific adhesion molecules phenotypes, Endothel. J. Endothel. Cell Res. 9 (2002) 247–261.
[37] J.S. Moreb, Aldehyde dehydrogenase as a marker for stem cells, Curr. Stem Cell Res. Ther. 3 (2008) 237–246.
[38] S. Akbari-Birgani, T. Paranjothy, A. Zuse, T. Janikowski, A. Cieslar-Pobuda, W. Likus, et al., Cancer stem cells, cancer-initiating cells and methods for their detection, Drug Discov. Today 21 (2016) 836–842.
[39] A. Cieslar-Pobuda, M.V. Jain, G. Kratz, J. Rzeszowska-Wolny, S. Ghavami, E. Wiechec, The expression pattern of PFKFB3 enzyme distinguishes between induced-pluripotent stem cells and cancer stem cells, Oncotarget 6 (2015) 29753–29770.
[40] K. Dang, K.A. Myers, The role of hypoxia-induced miR-210 in cancer progression, Int. J. Mol. Sci. 16 (2015) 6353–6372.
[41] M. Ivan, X. Huang, miR-210: fine-tuning the hypoxic response, Adv. Exp. Med. Biol. 772 (2014) 205–227.
[42] L.Z. Liu, C. Li, Q. Chen, Y. Jing, R. Carpenter, Y. Jiang, et al., MiR-21 induced angiogenesis through AKT and ERK activation and HIF-1alpha expression, PloS One 6 (2011) e19139.
[43] B. Yan, Q. Guo, F.J. Fu, Z. Wang, Z. Yin, Y.B. Wei, et al., The role of miR-29b in cancer: regulation, function, and signaling, Onco Targets Ther. 8 (2015) 539–548.